ARTICLE NO. 78-1180

# Mass Injection and Jet Flow Simulation Effects on Transonic Afterbody Drag

Wladimiro Calarese* and Ronald E. Walterick*
*Air Force Flight Dynamics Laboratory, Wright-Patterson AFB, Ohio*

**An experimental investigation has been performed on the effects of boattail injection and jet flow simulation on the afterbody drag of a slender body of revolution in the transonic regime at zero angle of attack. A correlation between sting and jet diameter has been established. The jet plume and the nozzle pressure ratio simulations have been found appropriate and useful as a testing technique. Boattail mass injection usually produces a drag coefficient reduction of 10-15% and is more effective at high nozzle pressure ratios and when used in regions of separated flow.**

## Nomenclature

$C_D$ = drag coefficient based on maximum cross-sectional area
$C_p$ = pressure coefficient, $\frac{p-p_\infty}{\gamma p_\infty M_\infty^2/2}$
$C_p^*$ = critical pressure coefficient
$\Delta C_p$ = pressure coefficient variation
$D$ = diameter
$L$ = length
$l$ = distance of frustrum from model base
$M$ = Mach number
$\dot{m}$ = mass flux
NPR = nozzle pressure ratio, $p_{oj}/p_\infty$
$p$ = static pressure
$p_o$ = stagnation pressure
$r$ = radius
$Re_L$ = Reynolds number based on model length
$S$ = cross-sectional area
$x$ = axial coordinate
$\beta$ = boattail average angle
$\beta_t$ = boattail terminal angle
$\phi$ = peripheral angle

*Subscripts*

$\beta$ = boattail
$b$ = base
$f$ = frustrum
$M$ = maximum
$s$ = sting
$A,j$ = afterbody, based on jet
$A,s$ = afterbody, based on sting
$\infty$ = infinity

## Introduction

IT is of utmost importance to develop new techniques capable of effectively reducing the afterbody drag of single-engine fighter or engine nacelles of aircraft performing in the transonic range. It has been ascertained that boattail and base injection when properly used, can reduce substantially the afterbody drag levels of slender bodies of revolution in the supersonic regime.[1,2] Consequently, an investigation was initiated in the Air Force Flight Dynamics Laboratory to determine whether the same effects would be obtained in the transonic regime. Preliminary results for boattail injection,[3] using a circular-arc boattail with a boattail average angle of 10 deg showed a favorable effect on the drag coefficient by injecting into the external flowfield small amounts of air in the freestream Mach number range 0.8-0.95. Additional experimental tests have been performed on boattails of different shapes and angles to confirm and validate the previous result and also to determine the effect of different parameters, such as location, area, and rate of injection as well as boattail shape and angle, nozzle pressure ratio, jet diameter, and Reynolds number. The testing technique of jet flow simulation by means of a cone frustum-sting combination was used in the experiment.

## Equipment and Test Description

The experiment was performed at the Trisonic Gasdynamic Facility of the Air Force Flight Dynamics Laboratory. A description of the facility can be found in Ref. 4. The tests were conducted at Mach 0.8-0.95, at a tunnel stagnation temperature of 500°R and stagnation pressures of 2000 and 3000 psf, which approximately correspond to Reynolds numbers of $8.3\times10^6$ and $13.4\times10^6$ based on the model length. The tests were performed at zero angle of attack on a sting-mounted, axisymmetric ogive-cylinder model with three

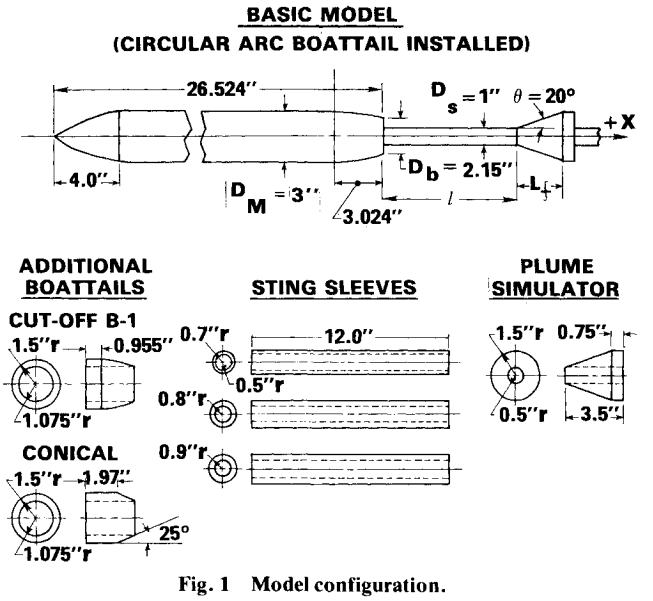


Fig. 1 Model configuration.

Presented as Paper 78-1180 at the AIAA 11th Fluid and Plasma Dynamics Conference, Seattle, Wash., July 10-12, 1978; submitted July 5, 1978; revision received Dec. 11, 1978. 

Index categories: Jets, Wakes, and Viscid-Inviscid Flow Interactions; Transonic Flow.

*Aerospace Engineer.

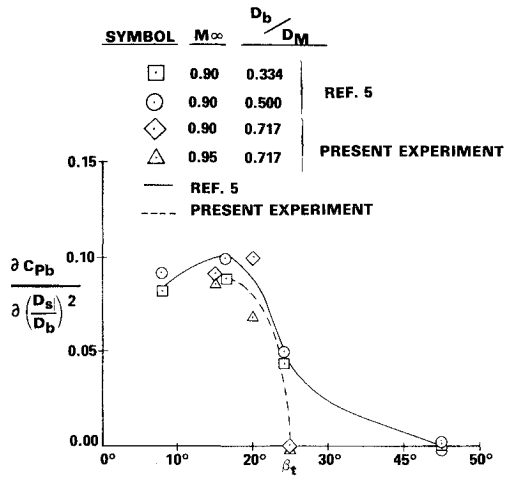


Fig. 2 Base pressure variation due to the sting vs terminal boattail angle.

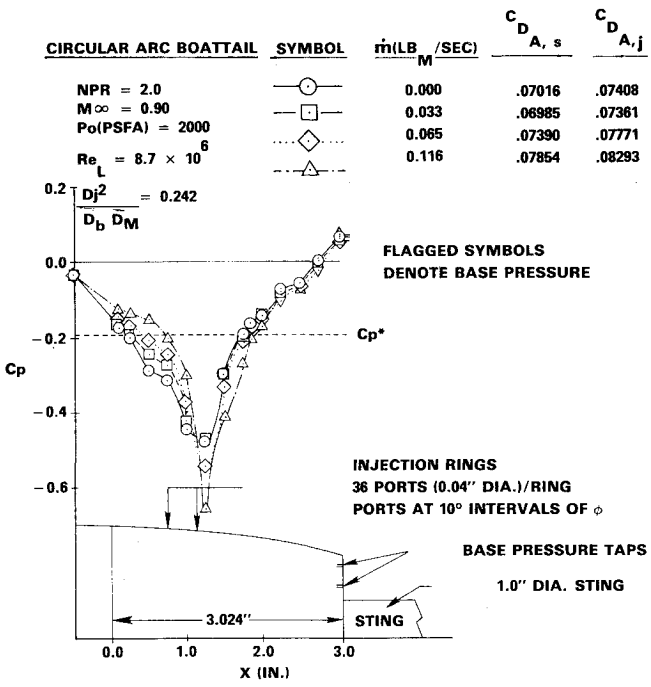


Fig. 3 Mass injection effect on circular-arc boattail and base pressure coefficients for NPR = 2.0, $D_s$ = 1 in.

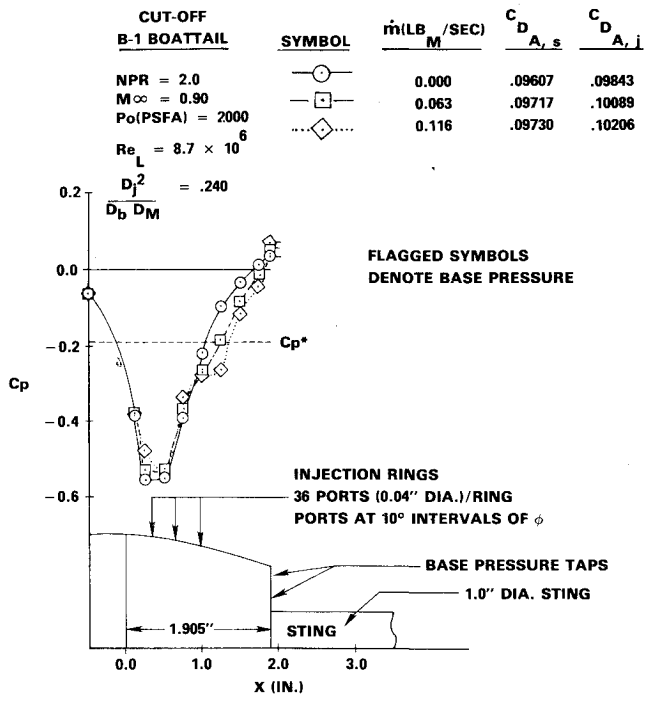


Fig. 4 Mass injection effect on cutoff B-1 boattail and base pressure coefficients for NPR = 2.0, $D_s$ = 1 in.

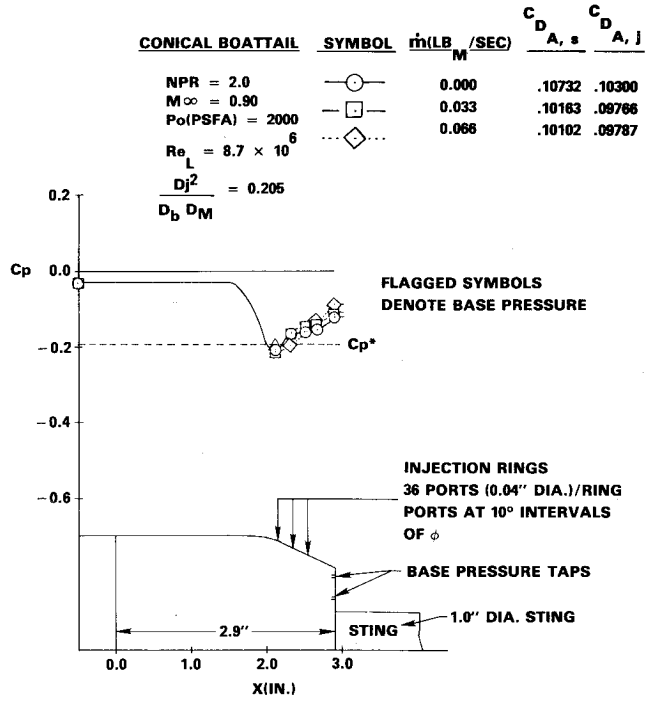


Fig. 5 Mass injection effect on conical boattail and base pressure coefficients for NPR = 2.0, $D_s$ = 1 in.

different boattails, i.e., a circular-arc, a cutoff version of the nozzle afterbody of the B-1 aircraft engine, and a conical boattail (Fig. 1). The boattails were equipped with 4-12 static pressure taps distributed circumferentially and longitudinally. Two additional pressure taps were located in the base region. Their base pressure measurements were slightly different from each other, but the pressure of the tap nearer to the base lip was used, since the other tap at times could not be used, as will be seen later.

The injection air was supplied through the rear sting to a settling chamber inside the boattail. The boattails were perforated at two or three different axial locations. The perforations consisted of 36 injection holes per location of 0.01 in. diam, distributed circumferentially at 10 deg intervals. The difference between the high pressure of the injection air and the low pressure of the external flow over the boattail produced the injection. The mass flux was regulated by a calibrated flow meter.

In Ref. 5, a correlation between the effects of the support sting-cone frustum combination on base pressure variation and the effects of a real jet plume was obtained. Based on this correlation, a cone frustum of 20 deg semivertex angle and 2.75 in. axial length was used as plume simulator and could be positioned over the support sting at different distances from the boattail end. The sting diameter could also be varied using sleeves of different diameters (Fig. 1). When the larger sleeves were applied, the base pressure tap nearer to the axis was covered and could not be used. The jet flow over a nozzle pressure ratio (NPR) of approximately 2, which represents a fully expanded sonic flow at the exit of a convergent nozzle, was simulated by the support sting without the frustum.

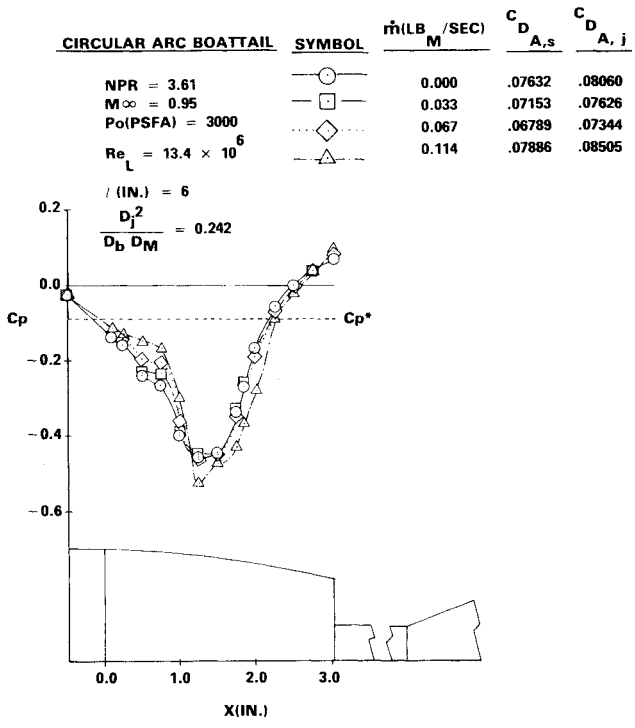


Fig. 6 Mass injection effect on boattail and base pressure coefficients for NPR > 2.

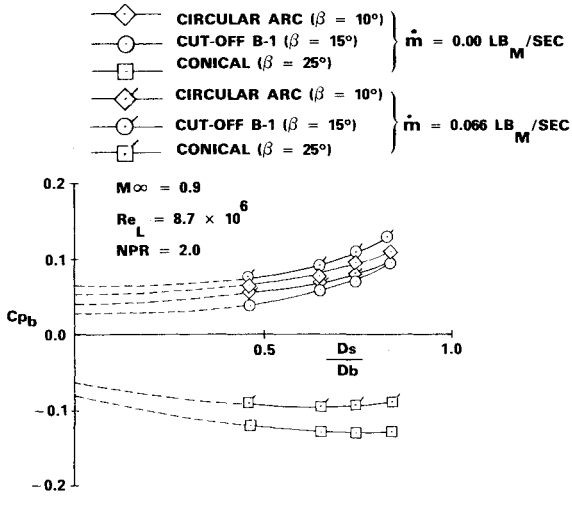


Fig. 7 Base pressure coefficient variation with sting size.

The base pressure variation due to the sting for constant model diameter

$$\Delta C_{ps} = \{\partial C_{pb}/\partial (D_s/D_b)^2\}(D_s/D_b)^2 \quad (1)$$

Similarly, the variation due to the jet is:

$$\Delta C_{pj} = \Delta C_{pb}(D_j^2 = 0) + \{\partial \Delta C_{pb}/\partial (D_j^2/D_b D_M)\} \times (D_j^2/D_b D_M) \quad (2)$$

The right-hand side terms of Eq. (2) have been obtained as functions of NPR by correlation with flight tests.[5] Since the sting must reproduce the same pressure variation as the jet, Eqs. (1) and (2) are equated, thus yielding a correspondence between sting and jet diameter.[6] The sting diameter $D_s$ is then obtained as an explicit function of the jet diameter $D_j$ and an implicit function of NPR for given values of $D_b$ and $D_M$.

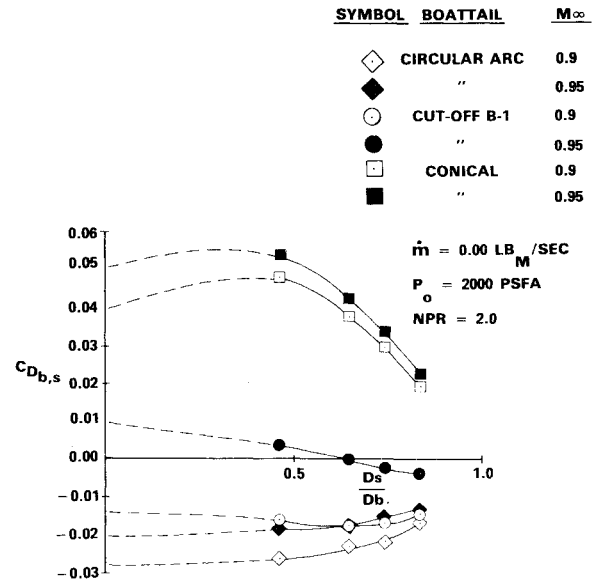


Fig. 8 Base drag coefficient variation with sting size.

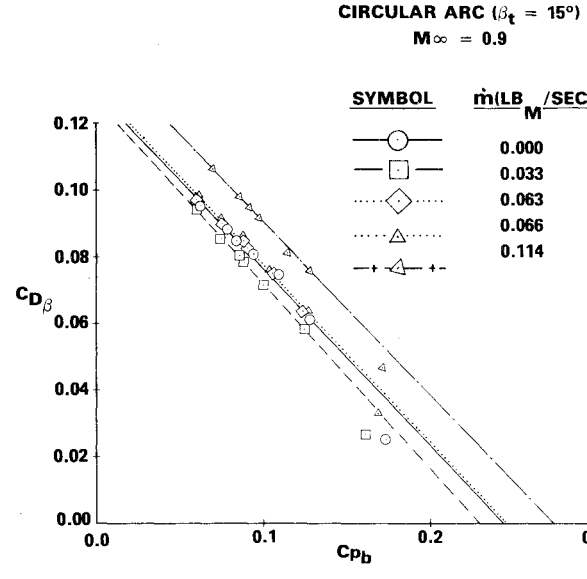


Fig. 9 Boattail drag coefficient variation with base pressure.

Note that the base pressure variation due to jet effects consists of two terms—one due to the jet flow; the other, $\Delta C_{pb}$ $(D_j^2 = 0)$, is the hypothetical contribution when the jet diameter is reduced to zero.

Even though the wind-tunnel simulation produces the same base pressure that a real jet would, the drag coefficient obtained with the sting is different from the one obtained with the jet due to the difference in the effective base area.

$$\frac{\Pi}{4}(D_b^2 - D_s^2) \neq \frac{\Pi}{4}(D_b^2 - D_j^2) \quad (3)$$

Then, in general,

$$C_{D_{A,s}} \neq C_{D_{A,j}} \quad (4)$$

Both drag coefficients are listed in Figs. 3-6, but the present parametric study is based mainly on the experimentally obtained value of $C_{D_{A,s}}$.

For NPR > 2, the simulation was accomplished by positioning the frustum on the sting at different distances from the model base while holding the sting diameter fixed.

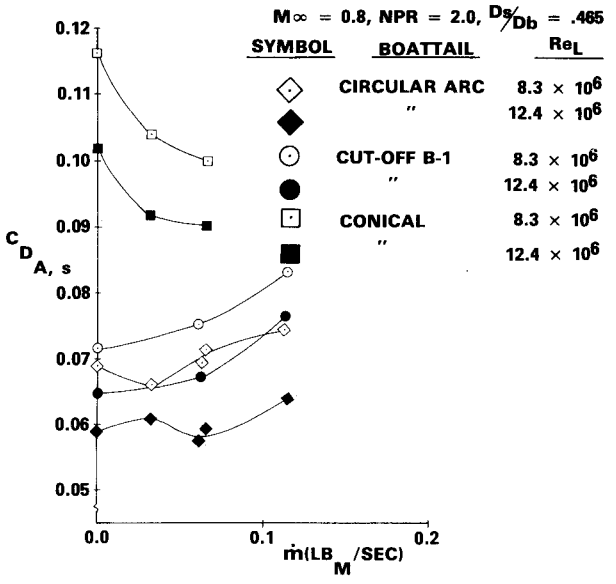


Fig. 10 Afterbody drag coefficient variation with mass injection for different Reynolds numbers, and NPR = 2, $M_\infty = 0.8$.

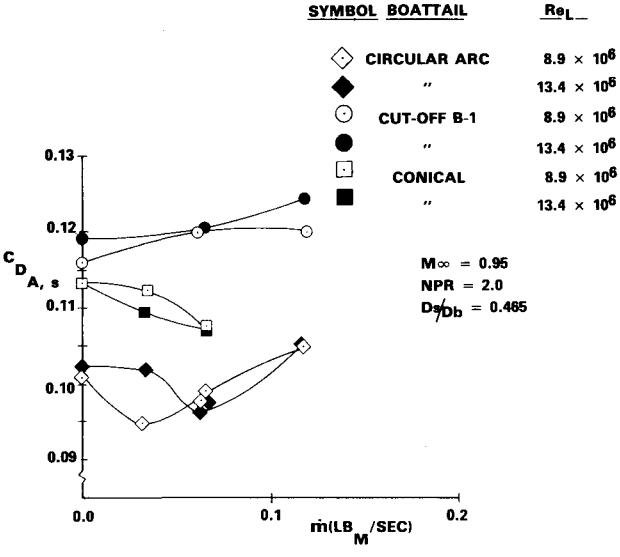


Fig. 11 Afterbody drag coefficient variation with mass injection for different Reynolds numbers, and NPR = 2, $M_\infty = 0.95$.

Reducing the frustum distance from the model base increases the NPR. The frustum is used to simulate the expanding jet plume. The effect of the frustum on the base pressure, given in Ref. 5, is obtained by adding to the right-hand side of Eq. (1) a term that is mainly a function of frustum semivertex angle, frustum length, and position.

The term $\partial C_{pb}/\partial(D_s/D_b)^2$ of Eq. (1) is a function of boattail angle and is plotted in Fig. 2 vs boattail terminal angle. Its value seems to have little dependence on $D_b/D_M$ and on Mach number in the range of the present experiment and is consistent with the value of Ref. 5, except for $\beta_t = 25$ deg (conical boattail). Conical boattails do not correlate well with simulation results obtained on different boattail shapes, especially when the boattail angle is high and separated flow occurs on the boattail.

## Results

Experimental data were obtained, reduced, and analyzed. The pressure coefficients for different configurations were plotted in order to investigate the effects of mass injection, Mach number, plume simulator, and sting diameter on the

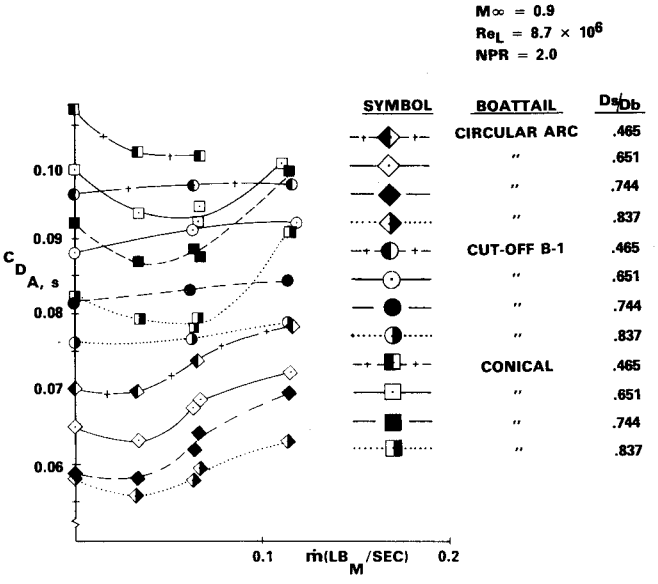


Fig. 12 Afterbody drag coefficient variation with mass injection for different sting sizes

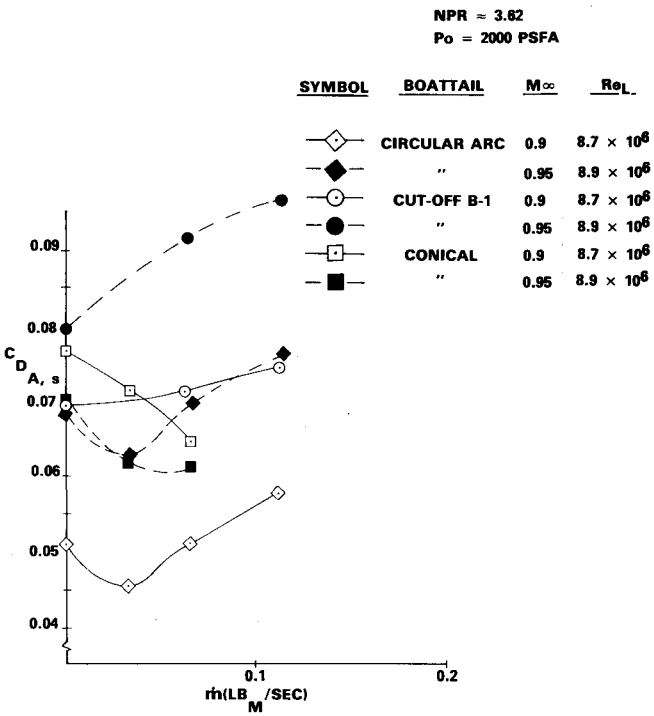


Fig. 13 Afterbody drag coefficient variation with mass injection for NPR = 3.62.

flowfield and on drag coefficient. The purpose of using different configurations, injection locations, and mass fluxes was to find those for which the overall integrated boattail and base pressure would give a drag reduction.

The afterbody drag coefficient based on the sting was calculated using the following equations:

$$C_{D_{A,s}} = C_{D_\beta} + C_{D_{b,s}} \tag{5}$$

where

$$C_{D_\beta} = \frac{1}{\bar{S}_M}\int_0^1 C_{p\beta}\bar{S}'_\beta \mathrm{d}\bar{x} \tag{6}$$

$$C_{D_{b,s}} = -C_{pb}(\bar{S}_b - \bar{S}_s)/\bar{S}_M) \tag{7}$$

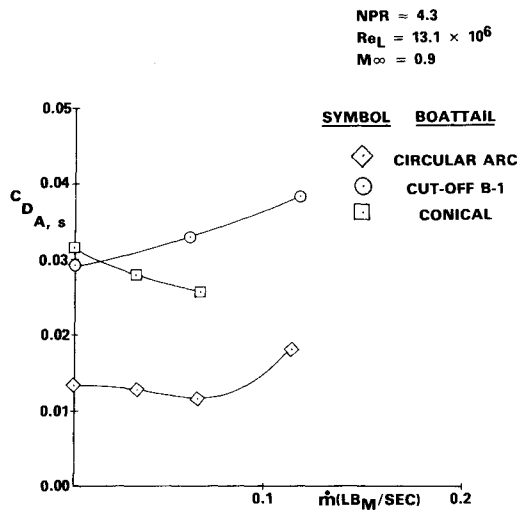


Fig. 14 Afterbody drag coefficient variation with mass injection for NPR = 4.3.

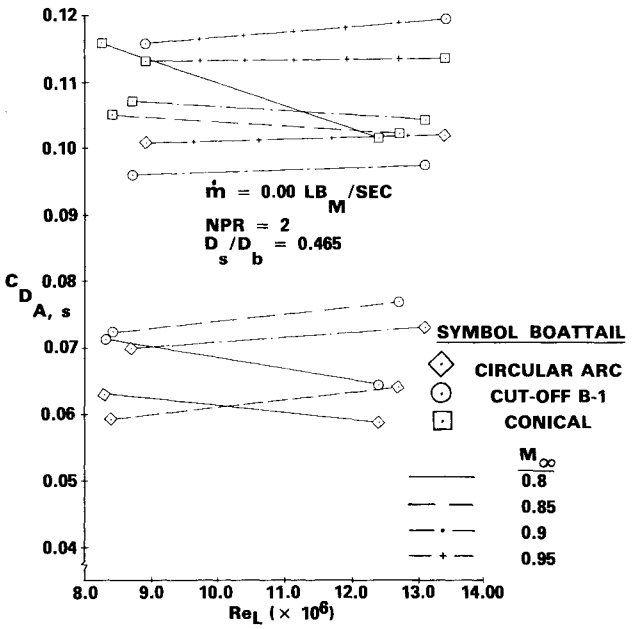


Fig. 15 Afterbody drag coefficient variation with Reynolds number.

where the prime superscript indicates first derivative with respect to $x$ and the bar superscript indicates quantities nondimensionalized with respect to the axial boattail length $L_\beta$.

If the jet flow is considered,

$$C_{D_{A,j}} = C_{D_\beta} + C_{D_{b,j}} \tag{8}$$

where

$$C_{D_{b,j}} = -C_{pb}(\bar{S}_b - \bar{S}_j)/\bar{S}_M \tag{9}$$

### A. Boattail Pressure Distribution

Figures 3-5 show the influence of mass injection on the pressure distribution and drag coefficient at a freestream Mach number of 0.9, a NPR of 2, and a sting diameter of 1 in. In general, the injection attenuates the expansion of the flow over the boattail shoulder ahead of the injection ports, but it degrades the recompression process on the terminal section of the boattail. The rate of injection is of critical importance in producing drag reduction or increase. In Fig. 3, for the circular-arc boattail, an injection rate of 0.033 lbm/s produces a

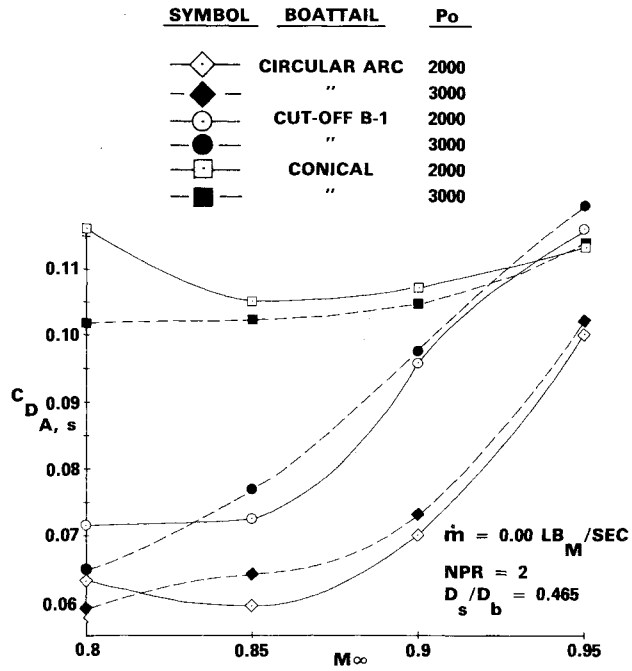


Fig. 16 Afterbody drag coefficient variation with freestream Mach number for NPR = 2.

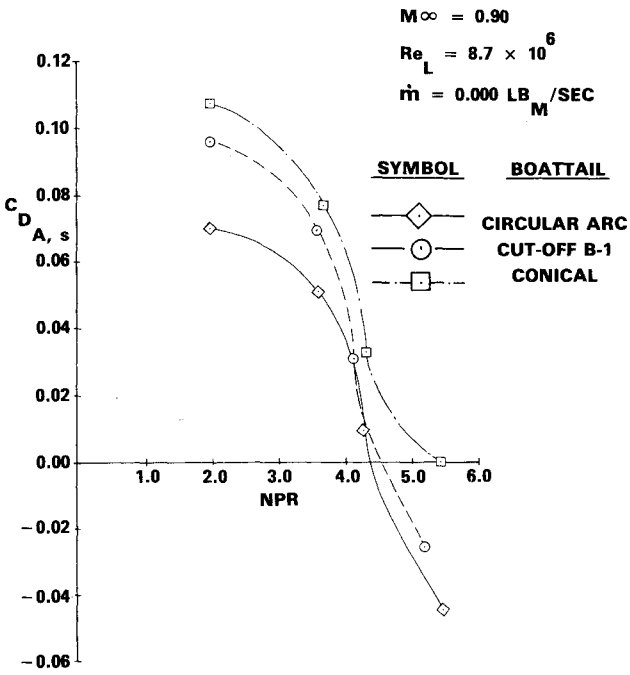


Fig. 17 Afterbody drag coefficient variation with nozzle pressure ratio without mass injection.

drag reduction while increasing the injection rate increases the drag. An examination of the pressure distribution shows that for the lower injection rates the injected flow produces a mild compression in front without causing a large separated region behind. The extent of the supersonic pocket is, therefore, reduced. At higher rates, the expansion over the boattail shoulder is at first favorably reduced but the expansion minimum reaches an even lower value. This lower value occurs immediately after the injection ports, revealing the occurrence of vortical flow with an extended separated region produced by the lateral jet issuing into the embedded supersonic field. Then, a stronger reattachment shock takes place.

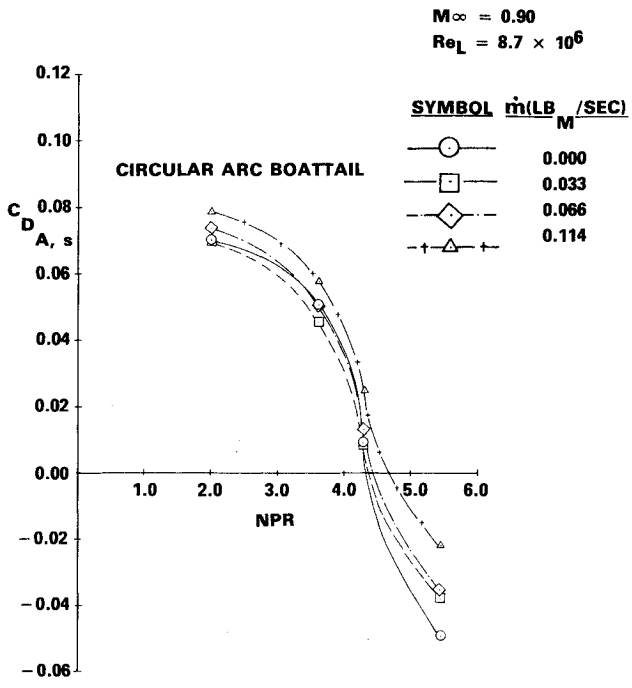


Fig. 18 Afterbody drag coefficient variation with nozzle pressure ratio for different mass injection rates.

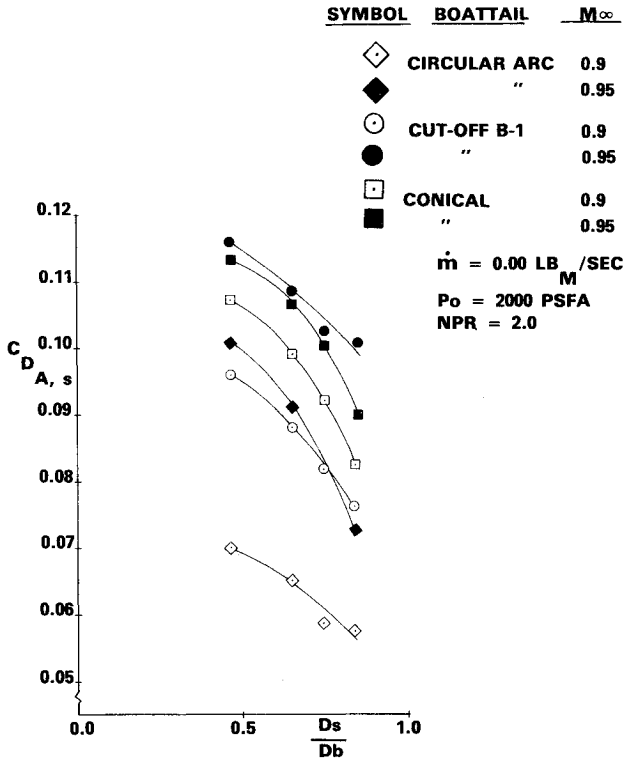


Fig. 19 Afterbody drag coefficient variation with sting size without mass injection.

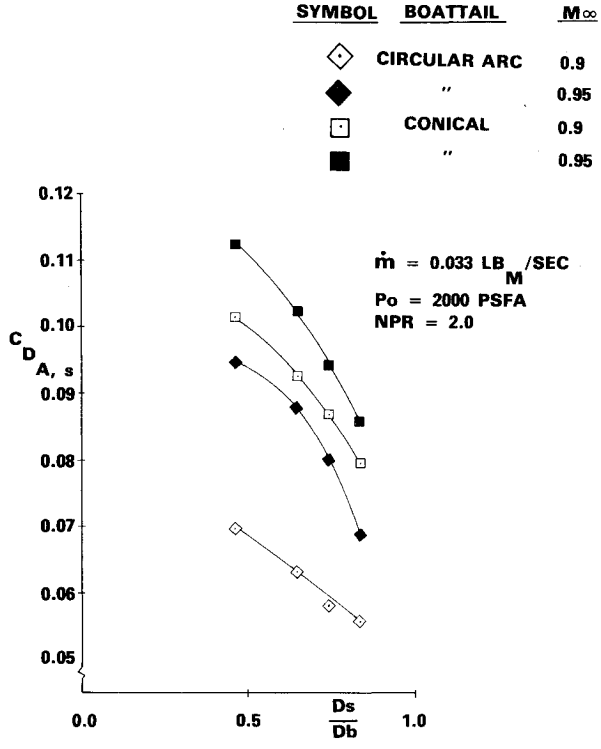


Fig. 20 Afterbody drag coefficient variation with sting size for $\dot{m}$ = 0.033 $lb_M/s$.

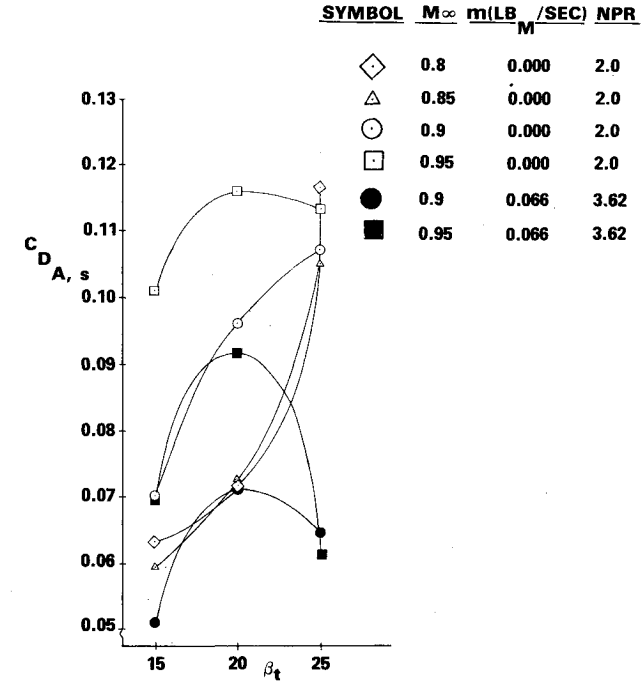


Fig. 21 Afterbody drag coefficient variation with boattail terminal angle.

A pattern somewhat different from the circular-arc boattail is seen in the pressure distribution of the cutoff B-1 (Fig. 4). In the case of supersonic flow occurring on the boattail when the mass injection is used, the extent of the supersonic pocket is larger than the one that develops on the circular-arc boattail because of the different location and area of injection, three rows of injection extending downstream to about 1 in. from the boattail end, while for the circular-arc only two rows extending downstream to about 2 in. from the boattail end (Fig. 3). The separation and reattachment shocks generated by the injection are farther apart, and the separated flow region is larger. Consequently, these phenomena produce stronger shock and separation losses and a drag increase with injection even though the base pressure at times rises with it.

The pressure distribution for the conical boattail is shown in Fig. 5. Because of the high boattail angle, $\beta$ = 25 deg, the flow is fully separated downstream of the boattail shoulder and no recompression occurs.

When mass injection is used, a drag reduction is obtained inasmuch as the injection energizes the flow in the separated region and delays separation; even though the expansion over the shoulder is bigger, a stronger recompression occurs downstream. As reported in Ref. 7, gas injection in a separated region is always beneficial for reducing the drag levels.

Figure 6 shows the pressure distribution on the circular-arc boattail for $M_\infty = 0.95$ and NPR = 3.61. The effect of the higher NPR consists of a better percentage drag reduction, about 10%, with small injection rates.

The mass injection rates that give the best drag reduction are between 0.03 and 0.06 lbm/s, which correspond to about 2-3% of the mass flow captured by a stream tube of area equal to the model's maximum cross-sectional area.

### B. Base Pressure Levels and Afterbody Drag Coefficients

Figure 7 shows how the base pressure is affected by the sting size. The base pressure coefficient increases with an increase in the value of $D_s/D_b$ for both the circular-arc and the cutoff B-1 boattails at any injection rate. It remains almost unchanged for the conical boattail. This happens because of the separated boattail flow caused by the high boattail angle. Consequently, its value is much lower than the value obtained for the other two boattails.

The base pressure values for zero sting diameter have been obtained by extrapolation and are indicated with dash lines. They are hypothetical and only indicative of the conditions that might exist in the base region in absence of the sting.

Figure 8 shows the corresponding base drag coefficients. At $\dot{m} = 0$, the circular-arc boattail exhibits a higher base thrust than the cutoff B-1. Instead, the conical boattail produces the highest base drag. The base drag curves tend obviously to zero when $D_s/D_b \to 1$.

Figure 9 illustrates a correlation between boattail drag coefficient and base pressure coefficient with and without mass injection at $M_\infty = 0.9$. The correlation for the circular-arc exhibits a higher negative slope than the McDonald-Hughes correlation[5] and is also slightly different when compared with the results of Ref. 3 (see Fig. 12 of Ref. 3). Nevertheless, the influence of the mass injection is well defined. Figure 9 first shows a boattail drag decrease with small injection rates, then an increase with higher injection rates for the circular-arc boattail.

Plots of the afterbody drag coefficient vs mass injection for NPR = 2.0 and different Reynolds numbers are reported in Figs. 10 and 11. The effect of boattail angle is evident in these figures. As expected at these high $\beta$'s, a higher boattail angle produces a higher drag coefficient because of the higher boattail shoulder expansion and lower subsequent recompression.

The conical boattail has the highest afterbody drag coefficient in Fig. 10 because of the high $\beta$ and the occurrence of separated flow downstream of the boattail shoulder, but is the most sensitive to mass injection. This injection produces considerable drag reduction. The circular-arc boattail shows a very small drag reduction with injection at $M_\infty = 0.8$, but the drag of the cutoff B-1 increases rapidly with injection. The drag reversal with injection (decrease-increase) is evident in the figures. The best configuration for lowest drag is the circular-arc, followed by the cutoff B-1, and then the conical boattail. Figure 10 shows a strong Reynolds number effect on the drag coefficient, but this was due to a defective pressure tap that gave incorrect readings for $Re_L = 8.3 \times 10^6$ (see Ref. 6). The drag variation due to the Reynolds number in Fig. 11 is not too strong. Its effect changes irregularly with the injection rates. No definite pattern is observed. It is interesting to note that at $M_\infty = 0.95$ the drag coefficient of the conical boattail is less than the one of the cutoff B-1. This effect is due to the early separation (right after the boattail shoulder) that the conical boattail experiences. This flow separation prevents the strong shoulder expansion from occurring.

Figure 12 is a plot of afterbody drag coefficient vs mass injection for various sting sizes. Again, the drag reversal with increasing $\dot{m}$ is observed. For each boattail configuration, the lowest drag coefficient is obtained with the maximum sting size. This result is due to two effects: 1) the reduction of effective base area which directly reduces the base drag and 2) the bigger sting simulates a higher jet flow and, therefore, a higher thrust, which better pressurizes the base region. The minimum overall drag is obtained for the circular-arc boattail, which also requires the lowest amount of mass injection to reach this minimum.

Figures 13 and 14 present the drag coefficient values with mass injection at NPR > 2. The favorable effect of mass injection for the circular-arc and conical boattails decreases with increasing NPR even though the drag levels decrease. This high NPR produces an adverse pressure gradient which, when added to the one generated by the injected flow, at times, causes an adverse interference. Note in Fig. 13 that the conical boattail produces less drag at $M_\infty = 0.95$ than at $M_\infty = 0.9$ for NPR = 3.62.

The Reynolds number effect on the drag coefficient for NPR = 2 and zero injection is shown in Fig. 15. Taking with reservation the high drag values for $M_\infty = 0.8$ and $Re_L \approx 8.3 \times 10^6$, due to the defective pressure tap mentioned before, it is evident that there is a small Reynolds number effect on the drag coefficient. For the circular-arc and cutoff B-1 boattails, there is a slight increase in drag with $Re_L$, while for the conical boattail, a slight decrease.

Figure 16 is a plot of $C_{D_{A_s}}$ vs $M_\infty$ for NPR = 2 and zero mass injection. The rate of drag increase with increasing $M_\infty$ is less for the conical than for the other boattails because of separation effects.

Figures 17 and 18 show that the increase of NPR considerably reduces the drag coefficient for any condition as expected, since it pressurizes the base region. The maximum decreasing rate occurs between NPR = 4 and 5.

The increase of the sting diameter also reduces the drag coefficient for any amount of mass injection as illustrated in Figs. 19 and 20. The reduction is considerable.

Finally, Fig. 21 shows the predicted increasing drag coefficient trend with boattail terminal angle for $M_\infty = 0.8$-0.9. For $M_\infty = 0.95$, the drag coefficient increases up to $\beta_t = 20$ deg, but then decreases because of the separation effects of the conical boattail which were discussed earlier. At higher NPR, the beneficial effect due to the injection in the separated region over the conical boattail is felt at $M_\infty = 0.9$ as well as $M_\infty = 0.95$. Consequently, the drag values drop considerably for $\beta_t = 25$ deg.

## Conclusions

An experimental investigation of the effects of boattail mass injection and jet flow on the transonic afterbody drag of slender bodies of revolution at zero angle of attack has been performed. The conclusions are:

1) A correlation between sting, used as jet simulator, and corresponding jet diameter has been established.

2) The jet plume and the NPR simulations by the sting-frustum combination have been found appropriate and useful and are considered a good testing technique.

3) Small rates of boattail mass injection, in general, produce a drag coefficient reduction and are more effective at high NPR's for the circular-arc and conical boattails. For the cutoff B-1 boattail, mass injection increases the drag levels in the present geometry. This boattail shape should not be used in conjunction with injection in this fashion. It is suggested that the injection port location should be re-examined in light of the present results and eventually replaced.

4) Mass injection is more effective in zones of separated flows.

5) For the boattail angle range used in the present report, 10-25 deg, the afterbody drag increases with increasing

boattail angle provided the boattail flow remains attached.

6) The conical boattail has the highest afterbody drag coefficient for $M_\infty$ = 0.8-0.9, NPR = 2, and no injection, but is the most sensitive to mass injection which produces considerable drag reduction. For $M_\infty$ = 0.95, the cutoff B-1 boattail exhibits the highest drag coefficient; the same is true when mass injection is considered at NPR > 2. In general, the circular-arc boattail gives the lowest drag values.

7) The Reynolds number has a negligible effect on the drag coefficient at NPR = 2 and zero injection.

8) The increase in Mach number produces a drag coefficient increase for all boattails at NPR = 2.

9) Concentrating the injection ports near the boattail shoulder attenuates the expansion at that location and produces a drag reduction for the circular-arc and conical boattails.

10) The NPR is very effective in changing the afterbody drag. An increase in NPR produces a substantial decrease in drag for all boattails.

11) Increasing the diameter of the sting, which simulates an increase in jet diameter, reduces the afterbody drag for all boattails.

## References

[1] Calarese, W. and Walterick, R.E., "GAU-8 Projectile Afterbody Drag Reduction by Base and Boattail Injection," AFFDL TM-77-27-FXM, March 1977.

[2] Freeman, L.M. and Korkegi, R.H., "Projectile Aft-Body Drag Reduction by Combined Boattailing and Base Blowing," AFFDL-TR-75-112, Feb. 1976.

[3] Calarese, W., Weeks, T.M., and Walterick, R.E., "Mass Injection and Jet Flow Simulation Effects on Boattail Drag in Transonic Flow," AFFDL TM-75-161-FXM, Nov. 1975.

[4] White, H.L., "Trisonic Gasdynamics Facility User Manual," AFFDL-TM-73-82-FXM, June 1973.

[5] McDonald, H. and Hughes, P.F., "A Correlation of High Subsonic Afterbody Drag in the Presence of a Propulsive Jet or Support Sting," *Journal of Aircraft,* Vol. 2, May-June 1965, pp. 202-207.

[6] Calarese, W. and Walterick, R.E., "Mass Injection and Jet Flow Simulation Effects on Transonic Afterbody Drag," AFFDL TM-77-95-FXM, Oct. 1977.

[7] Calarese, W., "An Analytical Method to Compute Viscous-Inviscid Transonic Flow on Axisymmetric Afterbodies Including Jet Effects and Boattail Bleed in Separated Regions," presented as Paper 75-1293 at the AIAA/SAE 11th Propulsion Conference, Anaheim, Calif., Sept. 24-Oct. 1, 1975.